Cumhuriyet Sci. J., 46(2) (2025) 396-404
DOI: https://doi.org/10.17776/csj.1626055

Cumhuriyet Science Journal

| csj.cumhuriyet.edu.tr | Founded: 2002 ISSN: 2587-2680 e-ISSN: 2587-246X Publisher: Sivas Cumhuriyet University

Optical Polarization Response of Hybrid Gratings Made of Metals and Polymers Based on Bruggeman Theory

Emirhan Taze[1,a], **Talha Erdem**[1,b,*]

[1] *Department of Electrical-Electronics Engineering, Abdullah Gül University, Kayseri 38080, Türkiye*

**Corresponding author*

Research Article

History
Received: 24/01/2025
Accepted: 20/06/2025

This article is licensed under a Creative Commons Attribution-NonCommercial 4.0 International License (CC BY-NC 4.0)

ABSTRACT

The current state of the art in grating designs has not adequately addressed compositions involving different metals and polymers. Our study aims to fill this gap by investigating how varying material compositions influence polarization properties. To explore this, we computed the refractive indices of hybrid mixtures containing gold, silver, and poly(dimethyl siloxane) (PDMS) using the Bruggeman effective medium theory. We then conducted simulations of optical transmission and reflection for gratings composed of these hybrid materials. Our analysis revealed distinct extinction coefficient peaks at specific wavelengths depending on the material ratios. Notably, our simulations indicate the possibility of fine-tuning the extinction coefficient within the spectral range of 450–1000 nm by modifying material composition. We also observed the ability to achieve polarization ratios of 0 and 1, demonstrating the potential for precise polarization control in optical applications. These findings suggest that carefully engineered metal-polymer hybrid gratings can serve as tunable optical filters and polarizers tailored to specific wavelength ranges. Customizing extinction properties and polarization response by varying the constituent materials provides new opportunities. Our results highlight the importance of material selection in grating design, paving the way for developing next-generation optical components with enhanced functionality.

Keywords: Hybrid nanomaterials, Optical polarization, Gratings, Effective medium approximation, FDTD.

[a] *emirhan.taze@agu.edu.tr* *https://orcid.org/0009-0007-4183-6954*
[b] *erdem.talha@agu.edu.tr* *https://orcid.org/0000-0003-3905-376X*

Introduction

A grating is a periodically varying structural or compositional system [1,2]. There are different types of gratings, depending on the periodicity direction and types. Such structures are employed in various applications including spectroscopy, optical polarizers, optical filtering, communication, ellipsometry, and lasers [1–7]. Their polarization-dependent reflection and transmission spectra [1,3,5,7–12] can be fine-tuned by controlling the period and duty cycle of the grating as well as by tailoring the material composition.

One of the promising class of structures utilizing gratings is metamaterials or metasurfaces [13,14]. Metasurfaces are periodic dielectric or optical structure which has unconventional optical properties such as linear [15] and circular [16] dichroism, negative refractive index, and total absorption characteristics [13]. These structures have periodicity in the sub-wavelength regime; in this regime, metallic nanoparticles have plasmonic characteristics causing strong wavelength-dependent responses [5,11]. Schnabel et al. showed a periodic thin metallic line on top of a dielectric surface where polarization-dependent transmission was observed [11]. Furthermore, Zhang et al. introduced plasmonic gratings made of gold nanowires with a tunable output band using solution-processed methods [5]. In recent years, soft materials have been employed together with these metallic plasmonic nanoparticles [13,14]. PDMS (Polydimethylsiloxane) is one of the widely used materials because of its stiffness, non-toxicity, inertness, and easy integration into the structures while SU-8 (Poly[(phenyl glycidyl ether)-co-formaldehyde)) and PEN (Polyethylene naphthalate) are among other alternatives [13]. Owing to their high elasticity [13,17], they find applications in transparent displays [17], tunable meta holograms [14], wearable biosensors in-vivo bioimaging with meta lens designs [14], deformation measurements [14,18], chiral spectroscopy and optomechanical MEMS devices [16]. In these works, soft materials were employed together with metals such as gold, silver, and aluminum [12,16–20] and achieved linear [19] and circular dichroism [16].

Thanks to the compatibility and scalable processing, plasmonic gratings made of gold or silver embedded in elastomers like PDMS have been widely studied in the literature [12–14,18–20]. In these works, polarization-dependent and/or independent wavelength-selective extinction characteristics have been demonstrated [12–14,16–20]. Nevertheless, a comprehensive analysis is missing to understand how the deformation or structural characteristics and material compositions affect linear dichroism.

To fill this gap in the literature, here, we want to reveal the potential optical performance of an exemplary hybrid system made of gold, silver, and poly (dimethyl siloxane) (PDMS). In our design, we first employed the Bruggeman

Theory [21–23] to calculate the effective refractive index of the composites. We then validated our results with the ellipsometry measurement data of gold and silver alloys in the literature [24]. Next, we modeled the gratings of composite materials having the calculated effective refractive indices as flat, thin stripes with varying periods and grating widths, and calculated polarization-dependent optical transmission and reflection using the Lumerical FDTD tool. Although the whole grating structure could have been modeled using an effective medium approximation, such an approach would lead to inaccurate results and remove polarization dependency because effective refractive index approximations perform better in randomly distributed systems [15].Therefore, here we preferred to model the composite material using Bruggeman theory and calculate the effect of grating structure using FDTD [15,19,21–23].Our simulation results revealed that employing metal and polymer compositions in gratings offers excellent wavelength selectivity in the polarization ratio of transmission and reflection. By adjusting material fractions and structural parameters, peak wavelength of polarization ratios could be adjusted between the wavelengths of 450 and 1000 *nm*. Furthermore, reaching 95% polarization ratios turn out to be possible.

After this brief introduction, in this article, we continue with the "Material and Method" section, where we explain the details of our calculations and the simulation parameters. These include the effective refractive index calculations and the geometrical design of the gratings and simulation structure. This section is followed by a "Results and Discussion" section which starts with the analysis of effective refractive index calculations followed by the electromagnetic simulation results on the polarization-dependent transmission and reflection characteristics of the gratings made of composite material system. Finally, we conclude by summarizing our key findings and presenting with a future outlook focusing on possible applications of our results.

Material and Method

Effective Refractive Index Calculations

We selected three materials, gold, silver, and poly (dimethyl siloxane) (PDMS), which will act as the building blocks of the hybrid stripes. Next, we calculated the effective refractive indices of these hybrids before running the electromagnetic simulations involving the stripes of these hybrids. Different methods for determining the effective refractive indices of hybrid materials have been developed in the literature. Each method is appropriate for a particular composition or type of material [21–23]. In this work, we preferred using the Bruggeman effective medium approximation since it is appropriate for modeling metal-based composites and widely employed in optical modeling [19,24] thanks to accurate optical response prediction in subwavelength-scale composite regions [21–23]. This model offers a useful and computationally efficient method to depict the average optical behavior of the composite regions before simulating their structured arrangement, even though it assumes an isotropic and random distribution of materials in bulk mixtures.

The entire grating structure was not directly simulated in our study using the Bruggeman model. Rather, it was used to calculate the local effective refractive indices of hybrid regions made of gold, silver, and PDMS. The periodic geometry was then explicitly considered in full-wave electromagnetic simulations using these estimates as input parameters. The validation of Bruggeman's theory approximation is carried out by comparing it with measurements obtained through ellipsometry, using the results of experimental results of Ref. [24].

In Eq. 1, the governing relation according to Bruggeman's theory is presented where f stands for the fraction of the first material, $1-f$ indicates the fraction of the second material, ε_{mix}, ε, ε_1 are the electric permittivity's of the mixture, the permittivity of the first material, and the permittivity of the second material, respectively.

$$f\,\frac{\varepsilon(\omega)\ -\ \varepsilon_{mix}(\omega)}{\varepsilon(\omega)\ +\ 2\varepsilon_{mix}(\omega)}+(1-f)\,\frac{\varepsilon_1(\omega)\ -\ \varepsilon_{mix}(\omega)}{\varepsilon_1(\omega)\ +\ 2\varepsilon_{mix}(\omega)}=0 \quad (1)$$

Rearranging the terms in Eq. 1 to find ε_{mix} results in a quadratic equation (Eq. 2) that has two solutions. We numerically calculated the roots of this equation using the NumPy library of Python and then employed the $n^2=\varepsilon$ relation to determine the effective refractive index *n*. To validate which solution is the effective refractive index, we used the Arago–Biot equation (Eq. 3) having a single solution [25,26] where *n* is the effective refractive index of the mixture, $\emptyset_i$ is the fraction of the i^{th} material, and n_i is the refractive index of the i^{th} material. We calculated the absolute difference between the roots of the Bruggeman theory and the Arago–Biot equation. We selected the root that minimizes the obtained result as the correct root.

$$\frac{2}{f-1}\times\varepsilon_{mix}(\omega)^2+\frac{3f-1}{f-1}\times\varepsilon_{mix}(\omega)\times\big(\varepsilon(\omega)-\varepsilon_1(\omega)\big)+\frac{1}{f-1}\times\varepsilon(\omega)\times\varepsilon_1(\omega)=0 \quad (2)$$

$$n=\sum_i \emptyset_i n_i \quad (3)$$

Since these equations can only design a mixture of two materials, we used them twice to calculate the refractive indices of the mixture made of different fractions of gold, silver, and PDMS. First, we designed different fractions of gold and silver according to the ratios. Then, we calculated the effective refractive index of the hybrid made of PDMS and the gold-silver mixture. PDMS fractions are varied from 0% to 40% with an increment of 2% while the remaining material was the gold-silver hybrid calculated in the previous step. In total, we calculated the effective refractive indices of 105 different material compositions.

Geometrical Design of the Gratings

Geometrical design of the gratings is illustrated in Figure 1. There are four distinct parameters that define these gratings. These are the effective refractive index of the hybrid material, the period of the gratings (*G*), the width of the stripes (*W*), and the height of the stripes (*H*). We kept the height parameter constant in our simulations at 20 *nm* and set the distance between gratings the same as the width of the stripes. This parameter changed between 150 *nm* to 250 *nm* in 10 *nm* intervals, as Table 1 shows.

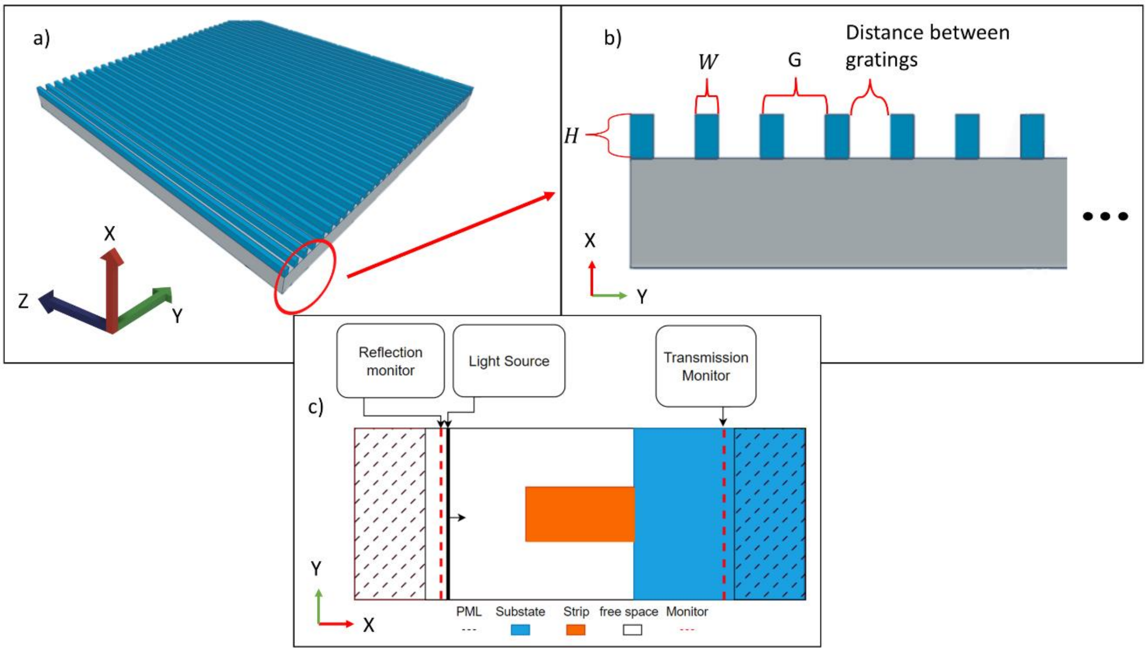

Figure 1. Representative image of the structure: (a) Isometric view and (b) side view of the structure. H, G, and W represent the height, period, and width of the gratings, respectively. (c) Illustration of the electromagnetic simulation setup in 2D.

Table 1. Geometrical parameters employed in simulations. Width (W), and period (G).

W	G
150 *nm*	300 *nm*
160 *nm*	320 *nm*
170 *nm*	340 *nm*
180 *nm*	360 *nm*
190 *nm*	380 *nm*
200 *nm*	400 *nm*
210 *nm*	420 *nm*
220 *nm*	440 *nm*
230 *nm*	460 *nm*
240 *nm*	480 *nm*
250 *nm*	500 *nm*

The electromagnetic simulations were carried out using Lumerical FDTD. Since we assumed infinitely long gratings, we ran the simulations in two dimensions, whereas y-axis and x-axis boundaries were set periodic and as perfectly matched layers (PML), respectively (Figure 1c). Further details of the simulation dimensions were presented in Supporting Information (SI). We recorded the reflected and transmitted power using a power monitor and the source was set as a plane wave whose polarization was set as 0° and 90°. The polarization ratio of the reflected and transmitted light was calculated using Eq. 4, where I_1 and I_2 stand for the recorded optical powers by the monitors at 0° and 90°, respectively.

$$Polarization\,ratio = \frac{|I_1 - I_2|}{I_1 + I_2} \tag{4}$$

Multiple convergence tests were conducted to optimize the computational cost (details are presented in the SI). The conventional uniform meshing was employed with the differential size being 1 *nm* (see the Supplementary File).

Results and Discussion

Refractive Indices of Hybrid Media

We calculated the refractive index values as explained in the methodology section. Figure 2 shows the real and imaginary parts of the calculated refractive indices for different fractions of gold and silver. Results reveal a gradual change of the refractive index as the fraction of the metals varies. We observe that by controlling the concentration of the metals involved, we can tailor the real and imaginary parts of the refractive index over a very broad spectral range, starting from the ultraviolet regime and extending to the infrared wavelengths. To confirm that Bruggeman's theory leads to similar results with experiments, we compared the calculated effective refractive indices with measurements obtained through ellipsometry for gold and silver mixtures presented in Ref.

[24]. Figure S1 shows a comparison of the calculated and measured refractive index of a gold-silver mixture. The calculated and measured refractive indices strongly resemble each other such that a mean squared error of only 0.032 and 0.015 are calculated for the real and imaginary parts of the refractive index, respectively. This rigorous validation process ensures the accuracy and reliability of our theoretical calculations.

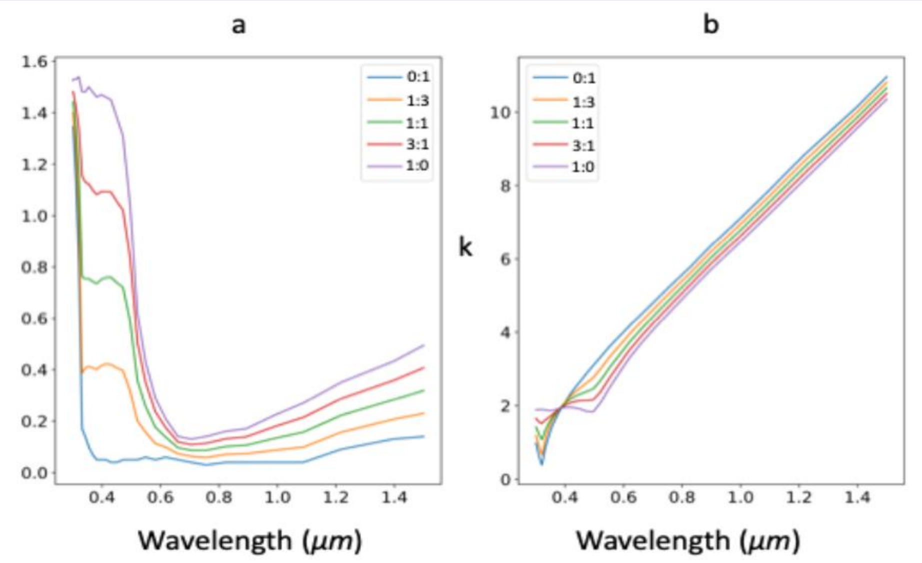

Figure 2. (a) Real and (b) imaginary parts of the refractive index belonging to the gold-silver mixture for different volume fractions. Legends are showing different concentrations of gold and silver. First number is gold fraction, second number is silver fraction.

After calculating the refractive index of hybrid material composed of gold and silver, we introduce PDMS as the third material. We calculated the refractive index of the final material systems by following the Bruggeman theory as described in the methods section. Results show that addition of PDMS decreases the extinction coefficient (k) and increase the real part of the refractive indices in the green-red regions of the spectrum (Figure 3). Furthermore, we observe that these variations are more prominent when silver is more dominant than gold in the mixtures.

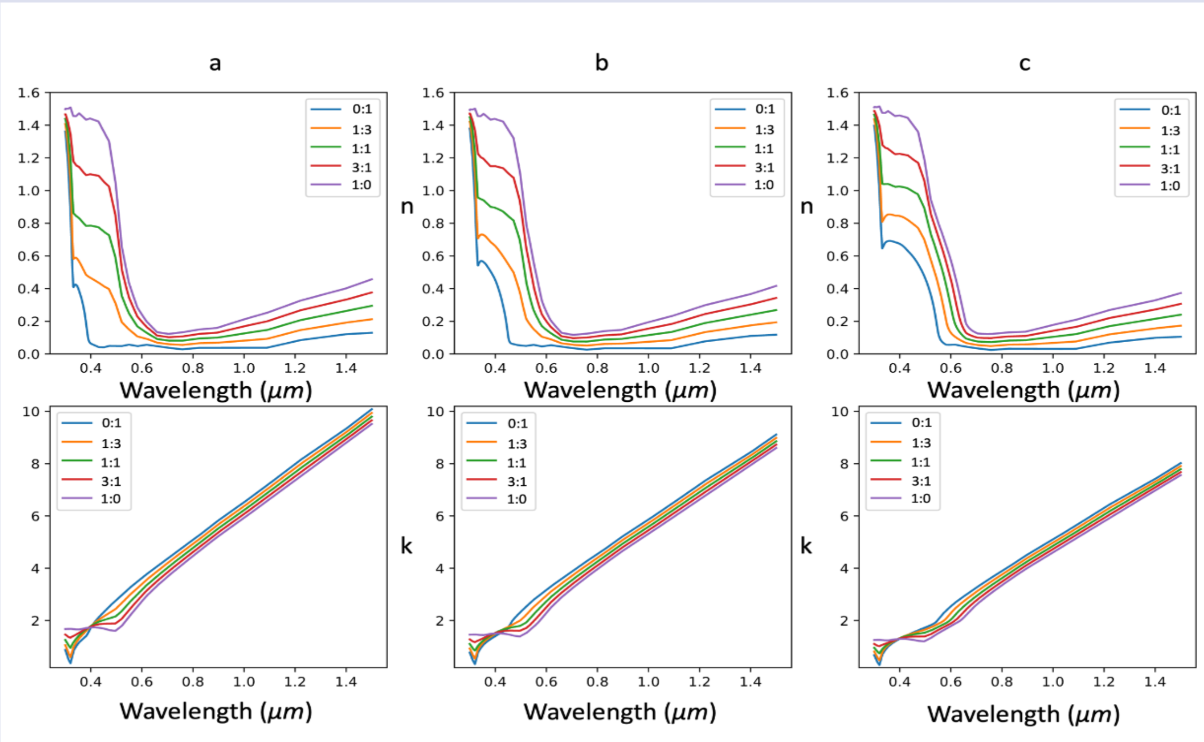

Figure 3. Real (n) and imaginary parts (k) of the refractive index belonging to hybrid materials composed of gold (G), silver (S), and PDMS (P) for different volume fractions. a) 10% PDMS used, b) 20% PDMS used, c) 30% PDMS used. Legends in the graphs show the ratio of Au - Ag concentration for the remaining part of the composition.

Analyses of polarization ratio in transmission spectra of the gratings

Composite materials are studied for use in tailoring the optical polarization of transmitted and reflected light in the gratings. In Figure 4, we present the polarization ratio of the light transmitted through gratings for different material compositions. Figure 4a shows polarization-dependent transmission spectra and Figure 4b shows polarization ratios of the transmitted light for a grating period of 300 *nm* and grating width of 150 *nm* without PDMS addition. Polarization-dependent transmission spectra belonging to the other structural parameters are given in Figure S2, and Figures S4-S24 present polarization ratios of the transmitted light both for remaining structural parameters and for all different material combinations. Results presented in Figure 4b and Figures S4-S24, which show the polarization ratio of the transmission results, indicate that there is always a single peak in the spectrum of the polarization ratio of the transmitted light. This peak appears because the transmission of the parallel polarized light takes its minimum value while the transmission of the vertically polarized light remains relatively high (Figure 4a). The characteristics of parallel polarized light are influenced by the material composition and structural parameters. Figures 4c and 4d show the effect of PDMS concentration in the material composition on the peak polarization ratio and its wavelength. Each point in Figure 4c corresponds to the wavelength at which the polarization ratio makes a peak for a single simulation, and Figure 4d indicates the corresponding peak polarization ratios. Results in Figure 4c indicate that by tailoring silver to gold ratio, the peak polarization wavelengths can be changed within an interval of ~200 nm for any PDMS ratio. Furthermore, increasing the PDMS ratio red shifts the polarization ratio peak wavelengths without changing the span of the wavelengths when the metal composition changes.

To quantify the effects of structural and material parameters on the peak polarization ratio and its wavelengths, we calculated their average and standard deviations for all the simulation parameters and analyzed how they change with respect to changes of a certain simulation parameter (Table 2). We observe that the peak polarization ratios of the transmission spectra take values close to unity. For most of the different material compositions, the peak point in the polarization ratio remains above 0.90.

On the other hand, the average wavelength where the peaks of polarization ratios appear is ~716 nm accompanied by a broad standard deviation of ~102 nm. Supporting our observation based on Figure 4, this indicates that gratings that have high polarization ratio response can be obtained over a broad spectral range by arranging the material and structural parameters. In Figure 4, we also observe that when the same material is used, minima of polarization ratios occur at slightly longer wavelengths than the peak polarization wavelengths.

Table 1. Average and standard deviations of peak polarization ratios and corresponding wavelengths for the transmitted light for all the material and structural parameters in addition to the polarization peak ratio wavelength shifts as gold concentration, PDMS concentration, and grating constant change. Detailed explanations how these analyses were made are presented in the SF.

Result Type	Average	Standard deviation
Polarization ratio’s peak wavelengths for all the material and structural parameter combinations	716.2 *nm*	101.6 *nm*
Polarization ratio’s peak values for all the material and structural parameter combinations	0.98	0.02
Silver-Gold concentration effect: The polarization peak wavelength shift per 1% Gold concentration increase for all the other material and structural parameters	1.03 *nm*	0.21 *nm*
PDMS concentration effect: The shift of the polarization peak wavelength per 2 %PDMS concentration increase for all the other material and structural parameters	15.2 *nm*	8.6 *nm*
Grating constant effect: The shift of the polarization peak wavelength per 20 nm increase in grating constant for all the other material and structural parameters	25.7 *nm*	4.5 *nm*

These minima typically take polarization ratio values below 0.10. This shows that such gratings can act as strong, polarization-dependent band-pass filters for light.

Analyses of the effect of the material composition also provides valuable insights (Table 2). Higher concentrations of gold in the gold-silver mixture result in a redshift in the polarization ratio of the transmission spectrum, per 1% increase in the gold concentration creates an average shift of 1.03 *nm* and a standard deviation of 0.21 *nm*. Gold, silver, and PDMS all contribute to this shift. The addition of PDMS to the composite extends the spectral coverage of the polarization ratio peaks into the red portion of the visible spectrum. Each 2% change in PDMS concentration causes the peak wavelength of the transmission spectrum to redshift by an average of 15.2 *nm*, with a standard deviation of 8.6 *nm*. A summary of how the polarization ratio of transmitted light varies as a function of PDMS concentration is presented in Figure 4d.

For the structural parameters, grating constant has an effect of 25.7 *nm* red shift of the peak location for each 20 *nm* change in the grating constant with 4.5 *nm* standard deviation. This shows that not only the material properties, but also the structural parameters are important to tailor the polarization ratio.

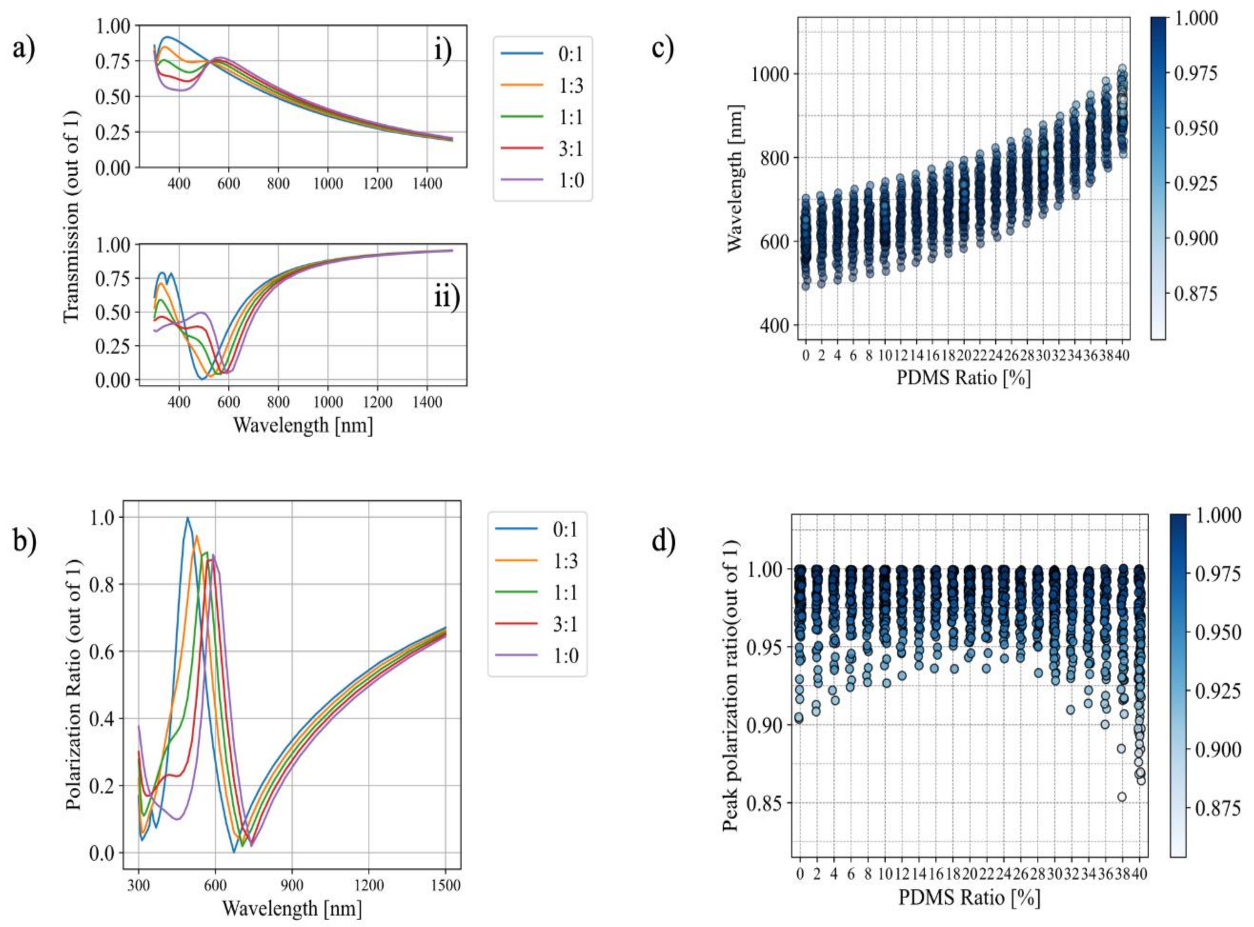

Figure 4. Polarization-dependent transmission response of the hybrid gratings made of silver, gold, and PDMS for a grating period of 300 nm and grating width of 150 nm. a) Transmission spectra belonging to the composites made of gold and silver at varying ratios without the addition of PDMS. i) parallel polarized light ii) perpendicular polarized light, legend shows gold: silver ratios. b) Polarization ratio of the transmission spectra belonging to the composites made of gold and silver at varying ratios without the addition of PDMS, legend shows gold: silver ratios. c) Peak wavelengths of the polarization ratio of transmission spectra for different PDMS fractions with respect to the gold and silver mixtures. d) Peak polarization ratio of transmission spectra for various PDMS fractions in gold and silver mixtures. The x-axis shows PDMS fractions, and the y-axis displays the corresponding peak values. Color heatmaps in c) and d) parts show the value of the peak polarization.

Analysis of Polarization Ratio in Reflection Spectra of the Gratings

In addition to the transmission, we analyzed the polarization-dependent reflection response of the gratings made of the hybrid materials. In Figure 5 and Table 3 we present results of polarization ratio of the reflected light for various material compositions and structural parameters. Figure 5a shows polarization-dependent reflection spectra and Figure 5b shows polarization ratios of the reflected light for a grating period of 300 *nm* and grating width of 150 *nm* without PDMS addition. Polarization-dependent reflection spectra belonging to the other structural parameters are given in Figure S3, and Figures S25-S45 present polarization ratios of the reflected light both for remaining structural parameters and for all different material combinations.

The calculated reflection spectra possess some general trends. Reflection of the s-polarized light exhibit minima, whereas the p-polarized light shows relatively higher reflection, resulting in sharp peaks in the polarization ratio calculations. As shown in Figure 5a, this mainly occurs due to strongly polarization-dependent reflection characteristics of silver and gold. As a result of these characteristics, polarization ratios make a valley in the ultraviolet regime. As the wavelength of interest gets longer, the polarization ratios first make a peak followed by a sharp valley in the red spectral region. In the infrared region, the polarization ratio increases further.

Figures 5c and 5d show the effect of PDMS concentration in the material composition on the peak polarization ratio and its wavelength. Each point in Figure 5c corresponds to the wavelength at which the polarization ratio makes a peak for a single simulation, and Figure 5d indicates the corresponding peak polarization ratios. In Table 3, we present our statistical analysis about the effects of structural and material parameters on the polarization ratio and its wavelengths. Results indicate that the peak polarization ratios can be obtained over a broad spectral range by tailoring the material compositions. On the other hand, the peak polarization ratios are around 0.67 with a low standard deviation, indicating that the peaks of the polarization ratios rarely can get larger values. Compared to the available polarization ratio peaks of the transmitted light, the potential values that can be obtained in the reflected light remain much lower.

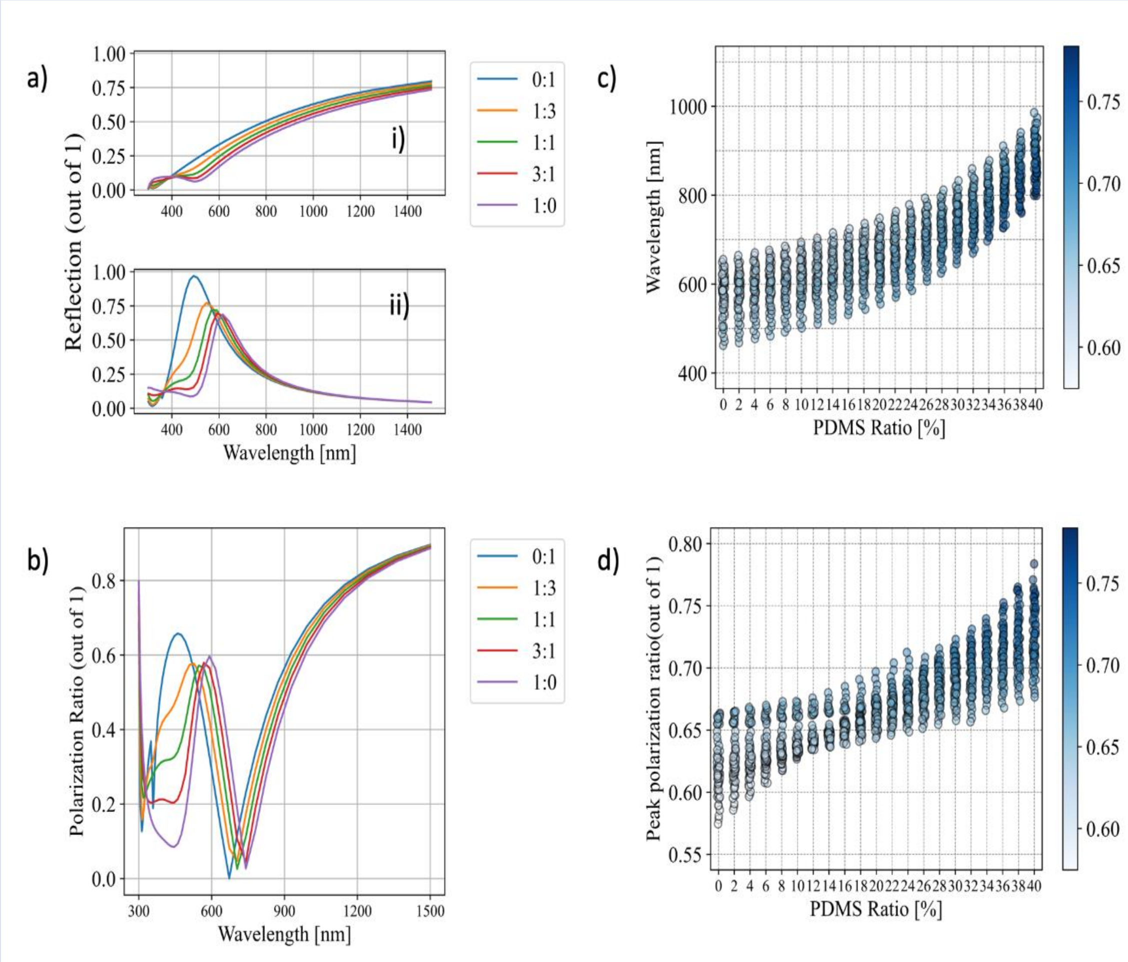

Figure 5. Polarization-dependent reflection spectra of the hybrid gratings made of silver, gold, and PDMS for a grating period of 300 nm and grating width of 150 nm. a) Reflection spectra of to the composites made of gold and silver at varying ratios without the addition of PDMS. i) parallel polarized light ii) perpendicular polarized light. Legend shows gold: silver ratios b) Polarization ratio spectra of the composites made of gold and silver at varying ratios without the addition of PDMS. Legend shows gold: silver ratios c) Peak wavelengths of the polarization ratio spectra of reflection for different PDMS fractions with respect to the gold and silver mixtures. d) Peak polarization ratios of reflection for various PDMS fractions in gold and silver mixtures. The x-axis shows PDMS fractions, and the y-axis displays the corresponding peak values. Color heatmaps in c) and d) parts show the value of the peak polarization.

We also analyzed how the change in the material and structural parameters affect the peak polarization ratios and their wavelengths. We calculated that for 1% change in the gold concentration, the wavelength of the peak polarization ratios red-shifts on average by 1.14 *nm* (±0.38 *nm*). The inclusion of PDMS in the material leads to a red shift in the polarization ratio peaks across the results. On average, each 2% change of PDMS concentration results in a shift of 15.3 *nm* (±9.31 *nm*).

Effect of structural parameters for the incident light reflection from the structure differs from the transmission results. For a grating constant change of 20 nm, the average wavelength of the peak polarization ratios red-shifts by 19.2 nm, with a standard deviation of 5.46 nm, which indicates a strong effect of grating constant on the wavelength at which the polarization ratio makes a peak

Given these findings, by carefully adjusting the amount of the materials and structural parameters, it becomes possible to tailor the peak wavelength of the polarization ratio for the reflected light over a broad spectral range. Simulations show different peak values for each of the polarization ratio peaks, and while the position can be adjusted, the highest amount of polarization peak ratio can be selected by meticulously choosing the ratios. Across all simulation results, the peak polarization ratios of the reflected light reach up to 0.78 while the minimum polarization ratio becomes 0.57 (Figure 5d).

Table 2. Statistical analysis of reflection spectra: Polarization ratio's peak values and the wavelengths where these peaks occur.

Result Type	Average Value	Standard deviation
Reflection polarization ratio's peak locations	684.75 *nm*	100.6 *nm*
Reflection polarization ratio's peak values (out of 1)	0.67	0.03
Silver-Gold concentration effect on the peak location shift for per 1% Gold concentration increase.	1.14 *nm*	0.38 *nm*
PDMS concentration effect on redshift of the peak location per 2 %PDMS concentration increase.	15.3 *nm*	9.3 *nm*
Grating constant effect on shift of the peak location per 20 nm increase in grating constant.	19.2 *nm*	5.5 *nm*

Conclusions

Unidirectional periodic structures exhibit distinct polarization-dependent characteristics. To expand the library of potential materials for polarizers, in this study, we analyzed the potential of gratings acting as linear polarizers made of hybrid materials containing gold, silver, and PDMS. We first calculated the refractive indices of these hybrids using Bruggeman and Arago-Biot theories followed by the electromagnetic simulations. In these simulations, gratings were formed with these hybrid materials, and the transmission and the reflection of the light was analyzed as a function of polarization.

The analyses of the polarization-dependent transmission spectra reveals that the polarization ratios can have maxima close to unity and minima close to zero for the same material and geometric configuration. This shows us that the gratings of these hybrid materials can act as strongly polarization-dependent optical band-pass filters. We also found out that increasing the gold content red-shifts the wavelength of the polarization ratio peak by ~1nm per 1% increase in the gold concentration. Addition of PDMS was found to have a more profound effect as it red-shifts the polarization peak by ~15 nm for an increase of 2% in the PDMS concentration. Furthermore, increasing the grating constant by 1 nm was found to red-shift the polarization ratio peak by ~1.3 nm.

The analyses of the reflection spectra show us that for all the composition combinations, the polarization ratio spectra have valleys in the ultraviolet regime. At longer wavelengths, a strong peak occurs followed by another valley, both of which fall in the visible regime. In the infrared regime the polarization ratio was found to take larger values. Compared to the polarization ratio of the transmitted light, that of the reflected light takes significantly lower values, which means that polarization-dependent absorption of the light plays a crucial role in obtaining high polarization ratios of the transmitted light.

The material-dependent polarization ratios of the reflected light have similar trends with the transmitted light, i.e., higher gold concentration red-shift the polarization ratio peaks and introducing PDMS results in more profound shifts of the polarization response. Furthermore, we found out that increasing grating-constant redshifts the wavelength at which the polarization ratio peak occurs.

Overall, our results show that with the hybrids of gold, silver, and PDMS, we can achieve strong polarization-dependent transmission and reflection characteristics. These effects turn out to be strongly wavelength-dependent, enabling polarization-dependent optical band-pass filters. Furthermore, we found out that selecting the correct material and geometrical properties for a desired polarization response is critical. We believe that these results can guide the design of hybrid polarizers and optical band-pass filters.

Acknowledgements

TE acknowledges the support from Tübitak 2247-A program Grant No. 120C124, from Science Academy (Bilim Akademisi) for BAGEP 2023 Award, and from the Turkish Academy of Sciences for the GEBİP Award. ET thanks YÖK 100/2000 program and Tübitak BİDEB 2211-A program.

Conflicts of interest

There are no conflicts of interest in this work.

References

[1] Palmer C., Loewen E., Diffraction grating handbook, 6th ed. New York (2005) 12-155.

[2] Loewen E., Popov E., Diffraction gratings and applications, 1st ed. New York (2018)

[3] Arkhipkin V. G., Myslivets S. A., One- and two-dimensional Raman-induced diffraction gratings in atomic media, *Phys Rev A (Coll Park)*, 98 (1) (2018) 013838.

[4] Knop K., Rigorous diffraction theory for transmission phase gratings with deep rectangular grooves, *JOSA* 68 (9) (1978) 1206-1210.

[5] Zhang X., Liu H., Tian J., Song Y., Wang L., Band-selective optical polarizer based on gold-nanowire plasmonic diffraction gratings, *Nano Lett*, 8 (9) (2008) 2653-2658

[6] Zhao L., Electromagnetically induced polarization grating, Scientific Reports, 8 (1) (2018) 1-10.

[7] Cincotti G., Polarization Gratings: Design and Applications, *IEEE J Quantum Electron*, 39 (12) (2003) 1645-1652.

[8] Wu J., Zhou C., Cao H., Hu A., Polarization-dependent and -independent spectrum selective absorption based on a metallic grating structure, *Opt Commun*, 309 (2013) 57-63.

[9] Ouyang M., Cao Y., Gao H., Shi J., Zhou J., Liu D., Analysis on polarization dependence of Fraunhofer diffraction by metallic grating with short period, *Opt Laser Technol*, 40 (1) (2008) 201-207.

[10] Sadov S. Yu., McGreer K. A., Polarization dependence of diffraction gratings that have total internal reflection facets, *JOSA A* 17 (9) (2000) 1590-1593.

[11] Schnabel B., Kley E.-B., and F. Wyrowski, “Study on polarizing visible light by subwavelength-period metal-stripe gratings,” *Opt. Eng.*, 38, (2) (1999) 220-226.

[12] Xu Y., Xu Y., Wang Y., Yang Y., Yang S., Li L., Xiang R., Xiang R., Liu J., Liu J, Stretchable structural colors with polarization dependence using lithium niobate metasurfaces, Optics Express, 32(4)(2024) 6776-6790.

[13] Chen Y., Ai B., Wong Z. J., Soft optical metamaterials, Nano Convergence, 7(1)(2020) 18.

[14] Effah E., Nettey-Oppong E. E., Ali A., Byun K. M., Choi S. H., Tunable Metasurfaces Based on Mechanically Deformable Polymeric Substrates, Photonics, 10(2)(2023) 119.

[15] Dolan J. A., Saba M., Dehmel R., Gunkel I., Gu Y., Wiesner U., Hess O., Wilkinson T. D., Baumberg J., Steiner U., Wilts B. D., Gyroid Optical Metamaterials: Calculating the Effective Permittivity of Multidomain Samples, ACS Photonics, 3(10)(2016) 1888-1896.

[16] Liu Z., Xu Y., Ji C., Chen S., Li X., Zhang X., Yao Y., Li J., Fano-Enhanced Circular Dichroism in Deformable Stereo Metasurfaces, Advanced Materials, 32(8)(2020) 1907077.

[17] Kumagai H.,Fujie T.,Sawada K.,Takahashi K, Stretchable and High-Adhesive Plasmonic Metasheet Using Al Subwavelength Grating Embedded in an Elastomer Nanosheet, Adv. Optical Mater.8 (15)(2020) 1902074.

[18] Li P., Gao K., Ma R., Pan K., Li D., Liu F., Li P., Gan X., Zhao J., Wen D., Stretchable plasmonic metasurfaces for deformation monitoring, Nanophotonics, 13(24)(2024) 4483-4490.

[19] Kim J., Kim H., Kim B., Chang T., Lim J., Jin H., Mun J., Choi Y., Chung K., Shin J., Fan S., Kim S., Highly tunable refractive index visible-light metasurface from block copolymer self-assembly, Nature Communications, 7(1)(2016) 1-9.

[20] Yoo D., Johnson T. W., Cherukulappurath S., Norris D. J., Oh S., Template-Stripped Tunable Plasmonic Devices on Stretchable and Rollable Substrates, ACS Nano, 9(11)(2015) 10647-10654.

[21] Bruggeman D. A. G, Berechnung verschiedener physikalischer Konstanten von heterogenen Substanzen. I. Dielektrizitätskonstanten und Leitfähigkeiten der Mischkörper aus isotropen Substanzen, *AnP*, 416 (7) (1935) 636-664.

[22] Gaponenko S. V., Nanoplasmonics I: metal nanoparticles. In: Gaponenko S. V., Introduction to Nanophotonics. 1st ed. New York: Cambridge University Press (2010) 166-198.

[23] Koledintseva M. Y., DuBroff R. E., Schwartz R. W., A Maxwell Garnett model for dielectric mixtures containing conducting particles at optical frequencies, *Progress in Electromagnetics Research*, 63 (2006) 223-242.

[24] Peña-Rodríguez O., Caro M., Olivares J., Perlado J. M., Rivera A., Caro A., Optical properties of Au-Ag alloys: An ellipsometric study, Optical Materials Express, 4(2)(2014) 403-410.

[25] An N., Zhuang B., Li M., Lu Y., Wang Z. G., Combined Theoretical and Experimental Study of Refractive Indices of Water-Acetonitrile-Salt Systems*, J Phys Chem B*, 119 (33) (2015) 10701-10709.

[26] Reis J. C. R., Lampreia I. M. S., Santos Â. F. S., Moita M. L. C. J., Douhéret G., Refractive Index of Liquid Mixtures: Theory and Experiment, *ChemPhysChem*, 11 (17) (2010) 3722-3733.